Sinopfbd, 2026; 11(1): 42-62 **https://doi.org/10.33484/sinopfbd.1624957**

Sinop Üniversitesi Fen Bilimleri Dergisi
Sinop Uni J Nat Sci
E-ISSN: 2564-7873

https://dergipark.org.tr/tr/pub/sinopfbd

Mathematical Modeling of Measles Outbreak with Two Patches

Tuğba AKMAN[1], Turgay KÜÇÜK[2] and Fikriye YILMAZ[3]

How to cite: Akman, T., Küçük, T., & Yılmaz, F. (2026). Mathematical modeling of measles outbreak with two patches. *Sinop Üniversitesi Fen Bilimleri Dergisi*, *11*(1), 42-62. https://doi.org/10.33484/sinopfbd.1624957

Open Access

Research Article

Corresponding Author
Tuğba AKMAN
takman@thk.edu.tr

ORCID of the Authors
T.A.: 0000-0003-1206-2287
T.K: 0000-0003-3424-2019
F.K.: 0000-0003-0002-9201

Received: 24.01.2025
Accepted: 24.12.2025

Abstract

In this study, single-patch and two-patch mathematical models are developed to investigate the progression of measles. First, the parameters of the single-patch model are estimated based on available data. The simulation results for the single-patch model show good agreement with real data. Additionally, the parameter values are used to construct a two-patch model that incorporates mutual migration or travel of both susceptible and infectious individuals between two countries. Then, the disease-free equilibrium points and the basic reproduction numbers for both models are obtained, and stability theorems are proven. The stability theorems are exemplified with simulations showing that the results align well with the theoretical findings.

Keywords: Mathematical modeling, measles, stability analysis, two-patch model

Kızamık Salgınının İki Yamalı Matematiksel Modellemesi

[1]University of Turkish Aeronautical Association, Department of Computer Engineering, Ankara, 06790, Türkiye

[2]National Defence University, Turkish Military Academy, Ankara, Türkiye

[3]Gazi University, Faculty of Science, Department of Mathematics, Ankara, Türkiye

Özet

Bu çalışmada, kızamık hastalığının seyrini araştırmak için tek yamalı ve iki yamalı matematiksel modeller geliştirilmiştir. İlk olarak, tek yamalı modelin parametreleri mevcut verilere dayanarak tahmin edilmiştir. Tek yamalı modelin simülasyon sonuçlarının, gerçek verilerle iyi bir uyum gösterdiği görülmüştür. Ek olarak, parametre değerleri, hem duyarlı hem de bulaşıcı bireylerin iki ülke arasında karşılıklı göçünü veya seyahatini içeren iki parçalı bir model oluşturmak için kullanılmıştır. Ardından, her iki model için hastalıksız denge noktaları ve temel üreme sayıları elde edilerek kararlılık teoremleri kanıtlanmıştır. Kararlılık teoremleri, sayısal sonuçların teorik bulgularla iyi uyum sağladığını gösteren simülasyonlarla örneklenmiştir.

Anahtar Kelimeler: Matematiksel modelleme, kızamık, kararlılık analizi, iki yamalı model

Introduction

Mathematical modeling has become an important tool to investigate the spread and transmission of infectious diseases, and there has been an increasing effort to construct new models and explore effective

intervention strategies to prevent the spread of a disease [1–12]. Measles, as a communicable viral infection, has a certain incubation period during which an individual remains in the latent infected class before moving to the infectious compartment [13]. In addition, an individual who contracted measles gains lifelong immunity [14]. Measles is lack of an antiviral treatment; but vaccination is very effective for prevention [15]. Mathematicians have investigated the dynamics of measles from different perspectives. For example, Edward et al. constructed a model consisting of susceptible, exposed, infected, vaccinated and recovered individuals, and found out that the spread of the disease depended on the transmission rate very strongly [16]. A disease model under the influence of environmental stress was constructed by Gürbüz et al. They incorporated fractional differential operators and solved the problem using the Adams-Bashforth-Moulton technique [17]. Işık et al. proposed a measles model to forecast measles in Turkey for the period 1970–2021 and they investigated practical identifibility of the model parameters [18]. In another recent study consdering the COVID-19 data of Turkey, a basic SEIR type model was developed and structural identifiability of the model was analyzed [19]. Roberts and Tobias developed a model for New Zealand in 1996 and this model successfully predicted the outbreak in 1997, and was used as an indicator to initiate a vaccination campaign [20]. Garba et al. developed a model of nine compartments, and they proposed that the model did not undergo backward bifurcation at the disease-free equilibrium point in case of a perfect vaccine [21]. İbrahim and Dénes proposed a model and applied it to the data in Pakistan from 2019 to 2021, and they underlined the importance of vaccination coverage [22]. A demographic model for Liverpool, U.K. was developed for 1863–1900 where living conditions were poor, and as a result, it was found that poor living conditions led to a large increase in the transmission coefficient in the model [23]. Kuddus et al. proposed a mathematical model using the cumulative number of confirmed measles cases in Bangladesh from 2000 to 2019, and the importance of mass vaccination was underlined [24]. On the other hand, a stochastic SVEIR model for measles with a Black–Karasinski process was developed to model the random effect in the dynamics [25]. As can be seen from studies in the literature, mathematical modeling of measles dynamics has been a very promising tool for many years. In this work, considering the characteristics of measles and motivated by the work [26], we propose a single-patch model for the spread of measles consisting of susceptible, vaccinated, exposed and infected subgroups. The parameter values for the single-patch model are obtained based on the measles data from Turkey in 2001 via data-fitting [27]. Then, based on the work of Tewa et al. [28], a two-patch mathematical model is constructed taking into account migration or travel between two countries. In this model, both susceptible and infectious individuals are allowed to migrate or travel mutually. The parameters values of the single patch model are then used in the two-patch model, since we do not have a data set reporting travel or migration of infected individuals. Furthermore, stability analysis is performed for both models. We present simulation results to illustrate theoretical findings of stability analysis, which align very well with the analytical results, and exemplify the effect of migration and disease transmission rates to the spread. The rest of the paper is organized as follows. In the section of mathematical models, two models are introduced. In the section of positivity and boundedness of the solutions, some proofs are presented for single and two-patch models. In the section of stability analysis, disease-free equilibrium points and the basic reproduction numbers of these models are found and analyzed. In the section of simulation results, numerical results are presented. Then, the paper ends with a summary and conclusion.

Mathematical Models

In this section, we develop two models for the transmission of measles with a single patch (excluding migration/travel) and two patches (considering migration/travel between two regions).

A Single-patch Model

A single-patch mathematical SVEIS model, motivated by the work of Sahu and Dhar [26], is constructed by splitting the total population of Turkey at time t, denoted $N := N(t)$, into four mutually exclusive compartments of individuals. The variables in the model represent the number of individuals in each compartment: susceptible $S := S(t)$, vaccinated $V := V(t)$, exposed $E := E(t)$ and infectious $I := I(t)$. Therefore, the total population is expressed as $N = S + V + E + I$. Susceptible individuals (S) become infected at the rate of β due to the interaction with infected individuals and they move to exposed subgroup. Two doses of measles vaccine have shown to provide immunity for 10–15 years [29], so vaccinated individuals become susceptible and move to the subgroup S at the rate of θ. On the other hand, susceptible individuals get vaccinated and move to the subgroup (V) at the rate of ω. Measles is associated with lifelong immunity [30]. Therefore, the vaccinated subgroup consists of both vaccinated individuals and recovered individuals due to life-long immunity gained due to measles. Recovered individuals join the subgroup V at the rate of γ, while some exposed individuals join the vaccinated subgroup at the rate of ξ due to natural immunity [26]. Exposed individuals are infected at the rate of σ. Infected individuals die at the rate of μ_d. In this model, unlike the model proposed by Sahu and Dhar [26], we construct an outbreak model, so newborns and recruitment of susceptible individuals are not included, and we assume that only infected individuals die. We ignore migration in the single patch model. In Figure 1, the transfer diagram showing the transition between the subgroups is given.

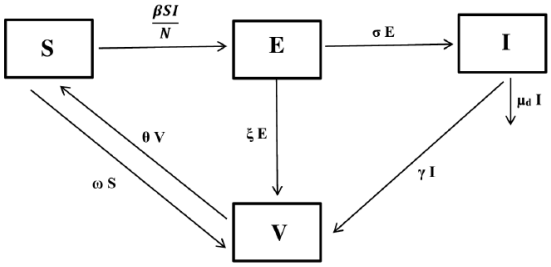

Figure 1. *Transfer diagram of the single patch model (1).*

Considering the assumptions and the transfer diagram above, the first model in this work is written as:

$$\begin{aligned}
\frac{dS}{dt} &= -\omega S + \theta V - \frac{\beta SI}{N}, \\
\frac{dV}{dt} &= \omega S - \theta V + \xi E + \gamma I, \\
\frac{dE}{dt} &= \frac{\beta SI}{N} - \xi E - \sigma E, \\
\frac{dI}{dt} &= \sigma E - \gamma I - \mu_d I,
\end{aligned} \tag{1}$$

with the non-negative initial conditions $S(0) = S_0, V(0) = V_0, E(0) = E_0, I(0) = I_0$.

A Two-patch Model

We proceed with a two-patch SVEIS model where we consider travel/migration of susceptible and infectious individuals between two neighboring countries, motivated by the work of Tewa et al. [28]. We note that in the work of Tewa et al., the authors include the travel of susceptible individuals between two patches. A similar model has been constructed in the work of Wessel by including death and birth terms in the model [31]. However, we consider an outbreak model, so we do not incorporate birth and natural death terms, and we use the parameters values obtained from a single patch model which is designed for an outbreak model as well. We assume that both susceptible and infectious individuals from two countries migrate or travel mutually. Therefore, we define new compartments S_i, E_i, V_i and I_i with $N_i = S_i + V_i + E_i + I_i$ for $i \in \{1, 2\}$ and extend the model (1). The subindex i is associated with the country i. The definition of the parameters in the model (1) is the same, except for the subindex i. Additional parameters used in the two-patch model are defined as α_1 (migration rate of susceptible individuals from the 1^{st} country to the 2^{nd} country), α_2 (migration rate of susceptible individuals from the 2^{nd}country to the 1^{st} country), α_3 (migration rate of infected individuals from the 1^{st} country to the 2^{nd} country) and α_4 (migration rate of infected individuals from the 2^{nd} country to the 1^{st} country). The transfer diagram of the two-patch model is given in Figure 2. We construct the model as

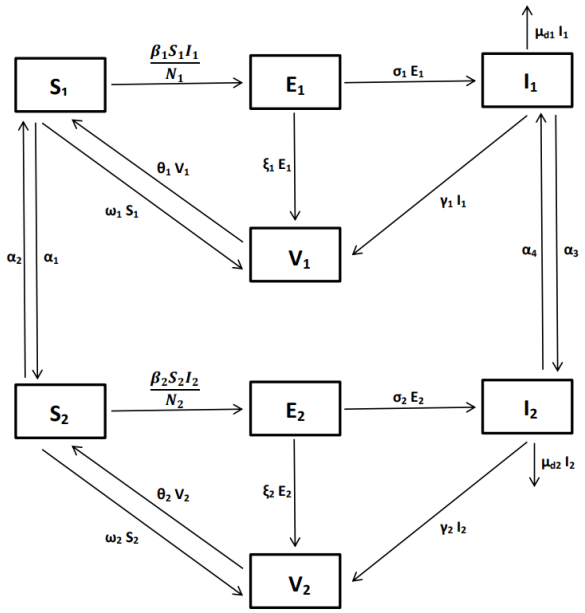

Figure 2. *Transfer diagram of the two-patch model (2).*

$$
\begin{aligned}
\frac{dS_1}{dt} &= -\omega_1 S_1 + \theta_1 V_1 - \frac{\beta_1 S_1 I_1}{N_1} - \alpha_1 S_1 + \alpha_2 S_2, \\
\frac{dV_1}{dt} &= \omega_1 S_1 - \theta_1 V_1 + \xi_1 E_1 + \gamma_1 I_1, \\
\frac{dE_1}{dt} &= \frac{\beta_1 S_1 I_1}{N_1} - \xi_1 E_1 - \sigma_1 E_1, \\
\frac{dI_1}{dt} &= \sigma_1 E_1 - \gamma_1 I_1 - \mu_{d1} I_1 - \alpha_3 I_1 + \alpha_4 I_2, \\
\frac{dS_2}{dt} &= -\omega_2 S_2 + \theta_2 V_2 - \frac{\beta_2 S_2 I_2}{N_2} + \alpha_1 S_1 - \alpha_2 S_2, \\
\frac{dV_2}{dt} &= \omega_2 S_2 - \theta_2 V_2 + \xi_2 E_2 + \gamma_2 I_2, \\
\frac{dE_2}{dt} &= \frac{\beta_2 S_2 I_2}{N_2} - \xi_2 E_2 - \sigma_2 E_2, \\
\frac{dI_2}{dt} &= \sigma_2 E_2 - \gamma_2 I_2 - \mu_{d2} I_2 + \alpha_3 I_1 - \alpha_4 I_2,
\end{aligned} \tag{2}
$$

with the non-negative initial conditions $S_1(0) = S_{1,0}$, $V_1(0) = V_{1,0}$, $E_1(0) = E_{1,0}$, $I_1(0) = I_{1,0}$, $S_2(0) = S_{2,0}$, $V_2(0) = V_{2,0}$, $E_2(0) = E_{2,0}$ and $I_2(0) = I_{2,0}$.

Positivity and Boundedness of the Solutions

We prove the theorems for the positivity and boundedness of the solution of Eqs. (1) and (2).

Theorem 1. Any solution $(S(t), V(t), E(t), I(t))$ of the system (1) with positive initial conditions is positive and bounded on $[0, T)$ with $T > 0$.

Proof. Let the initial conditions $S(0), V(0), E(0)$ and $I(0)$ be positive. We want to show that all variables in the model are positive for all $t > 0$. We first consider the variables $S(t)$ and $I(t)$. If both of them are positive for all t in $[0, T)$, then we are done. If not, there are values a_1 and a_2 such that $S(a_1) < 0$ and $I(a_2) < 0$ and we let a_1 and a_2 be the smallest values where $S(a_1) < 0$ and $I(a_2) < 0$. Now, let $a^* = \min(a_1, a_2)$. We examine two cases.

Case 1: Let $a^* = a_1$. Since $S(0) > 0$, it follows that there is a point t_1 such that $S(t_1) = 0$ and $S(t) > 0$ in $[0, t_1)$. Now, $I(t) > 0$ in $[0, t_1]$. We consider the third equation in (1),

$$
\frac{dE}{dt} = \frac{\beta S I}{N} - \xi E - \sigma E \geq -(\xi + \sigma) E, \quad \text{in } [0, t_1]. \tag{3}
$$

Integrating factor implies that

$$
\frac{dE}{dt} + (\xi + \sigma) E \geq 0 \Rightarrow E(t) \geq K \exp\left(- \int_0^t [\xi + \sigma] ds \right), \tag{4}
$$

where K is a constant. Then,

$$
E(t) \geq E(0) \exp\left(- \int_0^t [\xi + \sigma] ds \right) > 0. \tag{5}
$$

Now, we have $S(t) \geq 0, I(t) > 0$ and $E(t) > 0$ in $[0, t_1]$. Next, we consider

$$
\frac{dV}{dt} = \omega S - \theta V + \xi E + \gamma I \geq -\theta V. \tag{6}
$$

By a similar argument, we get $V(t) > 0$ in $[0, t_1]$. Then, the first equation is considered in $[0, t_1]$:

$$\frac{dS}{dt} = -\omega S + \theta V - \frac{\beta SI}{N} \geq -\left(\omega + \frac{\beta I}{N}\right) S. \tag{7}$$

By using an integrating factor, we get

$$S(t) \geq S(0) \exp\left(- \int_0^t [\omega + \frac{\beta I(s)}{N}] ds \right) > 0. \tag{8}$$

Then, at the point $t = t_1$,

$$S(t_1) \geq S(0) \exp\left(- \int_0^{t_1} [\omega + \frac{\beta I(s)}{N}] ds \right) > 0, \tag{9}$$

which is a contradiction to $S(t_1) = 0$. Thus, S cannot be negative.

Case 2: Let $a^* = a_2$. Similar arguments can be applied for the variable I as we have done above. We obtain that I cannot be negative. Since S and I are positive, we get $E > 0$ from the third equation in (1). Similarly, all variables must be positive in Eq.(1). After completing the first part of the theorem, we consider the total population $N = S + V + E + I$. If we add all equations in Eq.(1) up, we get

$$\frac{d(S + V + E + I)}{dt} = -\mu_d I \Rightarrow \frac{dN}{dt} = -\mu_d I, \Rightarrow N(t) \geq N(0) \exp(-\mu_d t). \tag{10}$$

Now, as $t \to \infty$, $N \to 0$. Also, $\frac{dN}{dt} = -\mu_d I < 0$ implies that N is decreasing and its largest value occurs at $t = 0$. Therefore, N is bounded. Thus, S, V, E and I are bounded, which completes the proof.

Theorem 2. Any solution $(S_1(t), V_1(t), E_1(t), I_1(t), S_2(t), V_2(t), E_2(t), I_2(t))$ of the system (2) with positive initial conditions is positive and is bounded on $[0, T)$ with $T > 0$.

Proof. Let the quantities $S_1(0), V_1(0), E_1(0), I_1(0), S_2(0), V_2(0), E_2(0)$ and $I_2(0)$ be positive. We want to show that all variables $S_1(t), V_1(t), E_1(t), I_1(t), S_2(t), V_2(t), E_2(t)$ and $I_2(t)$ are positive. We assume the opposite case: All variables has at least one negative value in $[0, T)$, say $S_1(a_1) < 0, V_1(a_2) < 0, E_1(a_3) < 0, I_1(a_4) < 0, S_2(a_5) < 0, V_2(a_6) < 0, E_2(a_7) < 0, I_2(a_8) < 0$, where a_i is the smallest value for each variable where the corresponding function attains its minimum. Since all initial values are positive, there must be some numbers $t_1, t_2, t_3, t_4, t_5, t_6, t_7$ and t_8 such that

- $S_1(t_1) = 0$ for $t_1 < a_1$ and $S_1(a_1) < 0$, $V_1(t_2) = 0$ for $t_2 < a_2$ and $V_2(a_2) < 0$, $E_1(t_3) = 0$ for $t_3 < a_3$ and $E_1(a_3) < 0$, $I_1(t_4) = 0$ for $t_4 < a_4$ and $I_1(a_4) < 0$,
- $S_2(t_5) = 0$ for $t_5 < a_5$ and $S_2(a_5) < 0$, $V_2(t_6) = 0$ for $t_6 < a_6$ and $V_2(a_6) < 0$, $E_2(t_7) = 0$ for $t_7 < a_7$ and $E_2(a_7) < 0$, $I_2(t_8) = 0$ for $t_8 < a_8$ and $I_2(a_8) < 0$.

We define $t^* = \min(t_1, t_2, t_3, t_4, t_5, t_6, t_7, t_8)$. We will examine all cases for t^* and try to get a contradiction to our assumption. If $t^* = t_1$, then $S_1(t^*) = 0$ and all variables are positive in $[0, t^*]$. Now, we consider the first equation in (2) on the interval $[0, t^*]$. Since $\theta_1 > 0$ and $\alpha_2 > 0$, it follows that

$$\frac{dS_1}{dt} = -\omega_1 S_1 + \theta_1 V_1 - \frac{\beta_1 S_1 I_1}{N_1} - \alpha_1 S_1 + \alpha_2 S_2 \geq -\left(\omega_1 + \frac{\beta_1 I_1}{N_1} + \alpha_1\right) S_1. \tag{11}$$

We integrate from 0 to t to get

$$S_1(t) \geq S_1(0) \exp\left(-\int_0^t [\omega_1 + \frac{\beta_1 I_1(s)}{N_1} + \alpha_1] ds \right) > 0. \tag{12}$$

Then, for $t = t^*$, we get

$$S_1(t^*) \geq S_1(0) \exp\left(-\int_0^{t^*} [\omega_1 + \frac{\beta_1 I_1(s)}{N_1} + \alpha_1] ds \right) > 0, \tag{13}$$

which is a contradiction to $S_1(t^*) = 0$. Similarly, if $t^* = t_2$, then $V_1(t^*) = 0$ and all variables are positive in $[0, t^*]$. Since $\omega_1 > 0, \xi_1 > 0$ and $\gamma_1 > 0$, we get a contradiction to $V_1(t^*) = 0$ as

$$V_1(t) \geq V_1(0) \exp\left(-\int_0^{t^*} [\theta_1] ds \right) > 0. \tag{14}$$

For the other variables, similar arguments are followed by using (2) and we get a contradiction. It means that $(S_1(t), V_1(t), E_1(t), I_1(t), S_2(t), V_2(t), E_2(t), I_2(t))$ must be positive in $[0, T)$. After completing the first part of the theorem, we consider the total population $N_1 = S_1 + V_1 + E_1 + I_1 + S_2 + V_2 + E_2 + I_2$. If we add all equations in the Eqn. (2) up, we get

$$\begin{aligned} \frac{d(S_1 + V_1 + E_1 + I_1 + S_2 + V_2 + E_2 + I_2)}{dt} &= -\mu_{d1} I_1 - \mu_{d2} I_2, \\ \Rightarrow \frac{dN_1}{dt} &= -\mu_{d1} I_1 - \mu_{d2} I_2, \\ \Rightarrow \frac{dN_1}{dt} &\geq -\max(\mu_{d1}, \mu_{d2})(I_1 + I_2). \end{aligned} \tag{15}$$

Let $\mu = \max(\mu_{d1}, \mu_{d2})$. Then, we get $\frac{dN_1}{dt} \geq -\mu N_1$. Now, we use the similar argument as in the previous theorem and obtain that $S_1(t), V_1(t), E_1(t), I_1(t), S_2(t), V_2(t), E_2(t)$ and $I_2(t)$ are bounded, which completes the proof.

Remark 1. We note that all partial derivatives of the functions on the right-hand side of the equations in (1) and (2) with respect to the model variables depend on the model variables and some constants, so these derivatives are bounded which implies the existence and uniqueness of the solution by the standard theory of ODEs.

Stability Analysis

A crucial question in infectious disease modeling is whether an emerging disease will spread in the population over time. This issue can be investigated with disease-free equilibrium points (DFE) and the basic reproduction number R_0 [5, 32]. In this section, we obtain the DFE points of the models (1)-(2), and then we perform stability analysis.

Stability analysis of the Single-patch Model

The DFE point of Eq.(1) is given by $P^0 = (S^0, V^0, 0, 0)$. Using $N = S + V + E + I$, we get $N = S^0 + V^0$. On the other hand,

$$0 = -\omega S^0 + \theta V^0 \Rightarrow V^0 = \frac{\omega S^0}{\theta}. \tag{16}$$

Now, substituting V^0 into this equation, we obtain

$$N = S^0 + \frac{\omega S^0}{\theta} \Rightarrow N\theta = S^0\theta + \omega S^0 \Rightarrow N\theta = (\theta + \omega)S^0 \Rightarrow S^0 = \frac{\theta N}{\theta + \omega}. \tag{17}$$

Inserting S^0 into V^0, we get

$$V^0 = \frac{\omega}{\theta}\left(\frac{\theta N}{\theta + \omega}\right) \Rightarrow V^0 = \frac{\omega N}{\theta + \omega}. \tag{18}$$

Therefore, the DFE point is found as

$$P^0 = \left(\frac{\theta N}{\theta + \omega}, \frac{\omega N}{\theta + \omega}, 0, 0\right). \tag{19}$$

Similarly, as in Van Den Driessche and Watmoug's study [32], the basic reproduction number is derived as

$$\frac{dX}{dt} = \mathcal{F} - \mathcal{V}, \quad \text{where} \tag{20}$$

$$\mathcal{F} = \begin{bmatrix} 0 \\ 0 \\ \frac{\beta SI}{N} \\ 0 \end{bmatrix} \quad \text{and} \quad \mathcal{V} = \begin{bmatrix} \omega S - \theta V + \frac{\beta SI}{N} \\ -\omega S + \theta V - \xi E - \gamma I \\ \xi E + \sigma E \\ -\sigma E + \gamma I + \mu_d \end{bmatrix}. \tag{21}$$

We denote the Jacobian matrices of $\mathcal{F}$ and $\mathcal{V}$ evaluated at the DFE point P^0 by F and V, respectively. Then, it follows that

$$F = \begin{bmatrix} 0 & \frac{\beta S^0}{N} \\ 0 & 0 \end{bmatrix}, \quad V = \begin{bmatrix} \xi + \sigma & 0 \\ \sigma & \gamma + \mu_d \end{bmatrix}. \tag{22}$$

The term FV^{-1} is called the next generation matrix [32] and it is given by

$$FV^{-1} = \begin{bmatrix} 0 & \frac{\beta S^0}{N} \\ 0 & 0 \end{bmatrix} \begin{bmatrix} \frac{1}{\xi+\sigma} & 0 \\ \frac{\sigma}{(\xi+\sigma)(\gamma+\mu_d)} & \frac{1}{\gamma+\mu_d} \end{bmatrix} = \begin{bmatrix} \frac{\beta S^0 \sigma}{N(\xi+\sigma)(\gamma+\mu_d)} & \frac{\beta S^0}{N(\gamma+\mu_d)} \\ 0 & 0 \end{bmatrix}. \tag{23}$$

The largest eigenvalue of FV^{-1} is $R_0 = \rho(FV^{-1})$, namely the basic reproduction number. It is written explicitly as

$$R_0 = \frac{\beta\theta\sigma}{(\theta + \omega)(\xi + \sigma)(\gamma + \mu_d)}. \tag{24}$$

Theorem 3. The DFE point of Eq.(1) is $P^0 = \left(\frac{\theta N}{\theta+\omega},\ \frac{\omega N}{\theta+\omega},\ 0,\ 0\right)$. We obtain the following results:

1. $R_0 = \frac{\beta\theta\sigma}{(\theta+\omega)(\xi+\sigma)(\gamma+\mu_d)} < 1 \Rightarrow P^0$ is asymptotically stable.
2. $R_0 = \frac{\beta\theta\sigma}{(\theta+\omega)(\xi+\sigma)(\gamma+\mu_d)} > 1 \Rightarrow P^0$ is unstable.

Proof. We have $V = N - S - E - I$. Inserting this in Eq.(1) yields

$$\begin{aligned}
\frac{dS}{dt} &= -\omega S + \theta(N - S - E - I) + \frac{\beta SI}{N}, \\
\frac{dE}{dt} &= \frac{\beta SI}{N} - \xi E - \sigma E, \\
\frac{dI}{dt} &= \sigma E - \gamma I - \mu_d I.
\end{aligned} \tag{25}$$

The Jacobian of Eq.(25) evaluated at the DFE point $P^0 = \left(\frac{\theta N}{\theta+\omega},\ \frac{\omega N}{\theta+\omega},\ 0,\ 0\right)$ is written as

$$J(P^0) = \begin{bmatrix} -\omega-\theta & -\theta & -\theta - \frac{\beta\theta}{\theta+\omega} \\ 0 & -\xi-\sigma & \frac{\beta\theta}{\theta+\omega} \\ 0 & \sigma & -\gamma-\mu_d \end{bmatrix}. \tag{26}$$

By rearranging the corresponding characteristic equation, we obtain

$$(-\omega-\theta-\lambda)[\lambda^2 + (\xi+\sigma+\gamma+\mu_d)\lambda + (\xi+\sigma)(\gamma+\mu_d)(1-R_0)] = 0. \tag{27}$$

The first eigenvalue is obtained as $\lambda_1 = -\omega - \theta < 0$. Other eigenvalues are the roots of the equation

$$\lambda^2 + (\xi+\sigma+\gamma+\mu_d)\lambda + (\xi+\sigma)(\gamma+\mu_d)(1-R_0) = 0. \tag{28}$$

Indeed, we have

$$\lambda_{2,3} = \frac{-(\xi+\sigma+\gamma+\mu_d) \pm \sqrt{(\xi+\sigma+\gamma+\mu_d)^2 - 4[(\xi+\sigma)(\gamma+\mu_d)(1-R_0)]}}{2}. \tag{29}$$

We investigate two different cases depending on the sign of R_0.

1. If $R_0 < 1$, then $\Delta \geq 0$ or $\Delta < 0$. If $\Delta \geq 0$, we have

$$\sqrt{(\xi+\sigma+\gamma+\mu_d)^2 - 4[(\xi+\sigma)(\gamma+\mu_d)(1-R_0)]} < \sqrt{(\xi+\sigma+\gamma+\mu_d)^2} = \xi+\sigma+\gamma+\mu_d \tag{30}$$

   Thus, both λ_2 and λ_3 are negative. The DFE point P^0 is locally asymptotically stable. On the other hand, if $\Delta < 0$, the real part of λ_2 and λ_3 is $-\frac{(\xi+\sigma+\gamma+\mu_d)}{2}$. Since ξ, σ, γ, μ_d are positive, λ_2 and λ_3 have negative real parts. Then, the DFE point of the model is locally asymptotically stable.

2. If $R_0 > 1$, then

$$\sqrt{(\xi+\sigma+\gamma+\mu_d)^2 - 4[(\xi+\sigma)(\gamma+\mu_d)(1-R_0)]} > (\xi+\sigma+\gamma+\mu_d), \tag{31}$$

so that λ_2 or λ_3 is positive. The DFE point P^0 is unstable.

Stability Analysis of the Two-patch Model

We start by finding the DFE point for the model (2). In the case of DFE, since all infected classes will be zero, we have $E_1 = E_2 = I_1 = I_2 = 0$. The DFE point of the system is obtained as

$$P^0 = (S_1^0,\, V_1^0,\, 0,\, 0,\, S_2^0,\, V_2^0,\, 0,\, 0). \tag{32}$$

Then, by using Eq. (32), the model (2) can be written as

$$\begin{cases} 0 = -\omega_1 S_1^0 + \theta_1 V_1^0 - \alpha_1 S_1^0 + \alpha_2 S_2^0, \\ 0 = \omega_1 S_1^0 - \theta_1 V_1^0, \\ 0 = -\omega_2 S_2^0 + \theta_2 V_2^0 + \alpha_1 S_1^0 - \alpha_2 S_2^0, \\ 0 = \omega_2 S_2^0 - \theta_2 V_2^0. \end{cases} \tag{33}$$

If we solve this system, we get

$$0 = \omega_1 S_1^0 - \theta_1 V_1^0 \Rightarrow V_1^0 = \frac{\omega_1 S_1^0}{\theta_1}. \tag{34}$$

By writing $N_1 = S_1 + V_1 + E_1 + I_1$, we obtain

$$N_1 = S_1^0 + V_1^0. \tag{35}$$

We substitute V_1^0 into (35) to obtain

$$N_1 = S_1^0 + \frac{\omega_1 S_1^0}{\theta_1} \Rightarrow N_1\theta_1 = S_1^0\theta_1 + \omega_1 S_1^0 \Rightarrow S_1^0 = \frac{\theta_1 N_1}{\theta_1 + \omega_1}. \tag{36}$$

Substituting S_1^0 into (34), we find

$$V_1^0 = \frac{\omega_1}{\theta_1}\left(\frac{N_1\theta_1}{\theta_1 + \omega_1}\right) \Rightarrow V_1^0 = \frac{\omega_1 N_1}{\theta_1 + \omega_1}.$$

After adding $-\omega_1 S_1^0 + \theta V_1^0 - \alpha_1 S_1^0 + \alpha_2 S_2^0 = 0$ and $\omega_1 S_1^0 - \theta V_1^0 = 0$ in Eq. (33), we get $\alpha_1 S_1^* = \alpha_2 S_2^0$. By inserting S_1^0, we have

$$\alpha_1\left(\frac{\theta_1 N_1}{\theta_1 + \omega_1}\right) = \alpha_2 S_2^0 \Rightarrow S_2^0 = \frac{\alpha_1\theta_1 N_1}{\alpha_2(\theta_1 + \omega_1)}. \tag{37}$$

Then,

$$0 = \omega_2 S_2^0 - \theta_2 V_2^0 \Rightarrow V_2^0 = \frac{\omega_2 S_2^0}{\theta_2}. \tag{38}$$

Inserting S_2^0, we get

$$V_2^0 = \frac{\omega_2\alpha_1\theta_1 N_1}{\theta_2\alpha_2(\theta_1 + \omega_1)}. \tag{39}$$

Since $\theta_1 = \theta_2$, $\omega_1 = \omega_2$, then

$$V_2^0 = \frac{\alpha_1 \omega_1 N_1}{\alpha_2(\theta_1 + \omega_1)}, \tag{40}$$

is obtained. Imposing $N_2 = S_2 + V_2 + E_2 + I_2$, we reach $N_2 = S_2^0 + V_2^0$. Substituting S_2^0 and V_2^0, we obtain

$$N_2 = \frac{\alpha_1 \theta_1 N_1}{\alpha_2(\theta_1 + \omega_1)} + \frac{\alpha_1 \omega_1 N_1}{\alpha_2(\theta_1 + \omega_1)} = \frac{\alpha_1 N_1(\theta_1 + \omega_1)}{\alpha_2(\theta_1 + \omega_1)} = \frac{\alpha_1 N_1}{\alpha_2}. \tag{41}$$

Thus, the DFE point is found as

$$P^0 = \left(\frac{\theta_1 N_1}{\theta_1 + \omega_1},\, \frac{\omega_1 N_1}{\theta_1 + \omega_1},\, 0,\, 0,\, \frac{\alpha_1 \theta_1 N_1}{\alpha_2(\theta_1 + \omega_1)},\, \frac{\alpha_1 \omega_1 N_1}{\alpha_2(\theta_1 + \omega_1)},\, 0,\, 0 \right). \tag{42}$$

Let $X = (E_1,\, E_2,\, I_1,\, I_2)$. Then, based on the work [5, 32], the model is written as

$$\frac{dX}{dt} = \mathcal{F} - \mathcal{V}, \tag{43}$$

where

$$\mathcal{F} = \begin{bmatrix} 0 \\ 0 \\ \frac{\beta_1 S_1 I_1}{N_1} \\ 0 \\ 0 \\ 0 \\ \frac{\beta_2 S_2 I_2}{N_2} \\ 0 \end{bmatrix}, \quad \mathcal{V} = \begin{bmatrix} \omega_1 S_1 - \theta_1 V_1 + \frac{\beta_1 S_1 I_1}{N_1} + \alpha_1 S_1 - \alpha_2 S_2 \\ -\omega_1 S_1 + \theta_1 V_1 - \xi_1 E_1 - \gamma_1 I_1 \\ \xi_1 E_1 + \sigma_1 E_1 \\ -\sigma_1 E_1 + \gamma_1 I_1 + \mu_{d1} I_1 + \alpha_3 I_1 - \alpha_4 I_2 \\ \omega_2 S_2 - \theta_2 V_2 + \frac{\beta_2 S_2 I_2}{N_2} - \alpha_1 S_1 + \alpha_2 S_2 \\ -\omega_2 S_2 + \theta_2 V_2 - \xi_2 E_2 - \gamma_2 I_2 \\ \xi_2 E_2 + \sigma_2 E_2 \\ -\sigma_2 E_2 + \gamma_2 I_2 + \mu_{d2} I_2 - \alpha_3 I_1 + \alpha_4 I_2 \end{bmatrix}. \tag{44}$$

Then, the Jacobian of $\mathcal{F}$ and $\mathcal{V}$ evaluated at the DFE point are written as

$$F = \begin{bmatrix} 0 & 0 & \frac{\beta_1 S_1^0}{N_1} & 0 \\ 0 & 0 & 0 & \frac{\beta_2 S_2^0}{N_2} \\ 0 & 0 & 0 & 0 \\ 0 & 0 & 0 & 0 \end{bmatrix}, \quad V = \begin{bmatrix} \xi_1 + \sigma_1 & 0 & 0 & 0 \\ 0 & \xi_2 + \sigma_2 & 0 & 0 \\ -\sigma_1 & 0 & \gamma_1 + \mu_{d1} + \alpha_3 & -\alpha_4 \\ 0 & -\sigma_2 & -\alpha_3 & \gamma_2 + \mu_{d2} + \alpha_4 \end{bmatrix}. \tag{45}$$

Based on the work of Salmani and Van Den Driessche [33], we can express F and V in terms of block matrices as

$$F = \left[\begin{array}{c|c} 0 & F_{12} \\ \hline 0 & 0 \end{array}\right], \quad V = \left[\begin{array}{c|c} V_{11} & 0 \\ \hline V_{21} & V_{22} \end{array}\right], \quad F_{12} = \begin{bmatrix} \frac{\beta_1 S_1^0}{N_1} & 0 \\ 0 & \frac{\beta_2 S_2^0}{N_2} \end{bmatrix}, \quad V_{11} = \begin{bmatrix} \xi_1 + \sigma_1 & 0 \\ 0 & \xi_2 + \sigma_2 \end{bmatrix},$$

$$V_{21} = \begin{bmatrix} -\sigma_1 & 0 \\ 0 & -\sigma_2 \end{bmatrix}, \quad V_{22} = \begin{bmatrix} \gamma_1 + \mu_{d1} + \alpha_3 & -\alpha_4 \\ -\alpha_3 & \gamma_2 + \mu_{d2} + \alpha_4 \end{bmatrix}. \tag{46}$$

In order to find the inverse of a matrix V, we define

$$V^{-1} = \left[\begin{array}{c|c} A & B \\ \hline C & D \end{array}\right]. \tag{47}$$

Then, we reach the partitioned matrix

$$VV^{-1} = \left[\begin{array}{c|c} V_{11} & 0 \\ \hline V_{21} & V_{22} \end{array}\right]\left[\begin{array}{c|c} A & B \\ \hline C & D \end{array}\right] = \left[\begin{array}{c|c} I_{11} & 0 \\ \hline 0 & I_{22} \end{array}\right]. \tag{48}$$

From Eq. (48), we arrive at the following term:

$$\begin{array}{l} V_{11}A = I_{11} \Rightarrow A = V_{11}^{-1}, \quad V_{11}B = 0 \Rightarrow B = 0, \\ V_{21}B + V_{22}D = I_{22} \Rightarrow V_{22}D = I_{22} \Rightarrow D = V_{22}^{-1}, \\ V_{21}A + V_{22}C = 0 \Rightarrow V_{22}C = -V_{21}A \Rightarrow V_{22}C = -V_{21}V_{11}^{-1} \Rightarrow C = -V_{22}^{-1}V_{21}.V_{11}^{-1} \end{array}, \tag{49}$$

Substituting $A,\ B,\ C,\ D$ in (47), we obtain

$$V^{-1} = \left[\begin{array}{c|c} V_{11}^{-1} & 0 \\ \hline -V_{22}^{-1}V_{21}.V_{11}^{-1} & V_{22}^{-1} \end{array}\right]. \tag{50}$$

Then,

$$FV^{-1} = \left[\begin{array}{c|c} 0 & F_{12} \\ \hline 0 & 0 \end{array}\right]\left[\begin{array}{c|c} V_{11}^{-1} & 0 \\ \hline -V_{22}^{-1}V_{21}.V_{11}^{-1} & V_{22}^{-1} \end{array}\right] = \left[\begin{array}{c|c} -F_{12}V_{22}^{-1}V_{21}.V_{11}^{-1} & F_{12}V_{22}^{-1} \\ \hline 0 & 0 \end{array}\right], \tag{51}$$

is obtained. The largest eigenvalue of FV^{-1}, namely the basic reproduction number, is found as $R_0 = \rho(FV^{-1}) = \rho(-F_{12}V_{22}^{-1}V_{21}V_{11}^{-1})$. Now, our aim is to express the term $V_{22}^{-1}V_{21}V_{11}^{-1}$ in terms of the parameters explicitly. We note that matrices V_{11}^{-1} and V_{22}^{-1} are computed as

$$V_{11}^{-1} = \frac{1}{(\xi_1+\sigma_1)(\xi_2+\sigma_2)}\begin{bmatrix} \xi_2+\sigma_2 & 0 \\ 0 & \xi_1+\sigma_1 \end{bmatrix} = \begin{bmatrix} \frac{1}{\xi_1+\sigma_1} & 0 \\ 0 & \frac{1}{\xi_2+\sigma_2} \end{bmatrix}, \tag{52}$$

$$V_{22}^{-1} = \frac{1}{(\gamma_1+\mu_{d1}+\alpha_3)(\gamma_2+\mu_{d2}+\alpha_4)-\alpha_3\alpha_4}\begin{bmatrix} \gamma_1+\mu_{d1}+\alpha_3 & \alpha_4 \\ \alpha_3 & \gamma_2+\mu_{d2}+\alpha_4 \end{bmatrix}. \tag{53}$$

Then, the matrix $-F_{12}M$, with $M = V_{22}^{-1}V_{21}V_{11}^{-1}$, can be written as

$$-F_{12}V_{22}^{-1}V_{21}V_{11}^{-1} = \begin{bmatrix} \frac{\beta_1\theta_1(\gamma_2+\mu_{d2}+\alpha_4)\sigma_1}{(\theta_1+\omega_1)((\gamma_1+\mu_{d1}+\alpha_3)(\gamma_2+\mu_{d2}+\alpha_4)-\alpha_3\alpha_4)(\xi_1+\sigma_1)} & \frac{\beta_1\theta_1\alpha_4\sigma_2}{(\theta_1+\omega_1)((\gamma_1+\mu_{d1}+\alpha_3)(\gamma_2+\mu_{d2}+\alpha_4)-\alpha_3\alpha_4)(\xi_2+\sigma_2)} \\ \frac{\beta_2\theta_1\alpha_3\sigma_1}{(\theta_1+\omega_1)((\gamma_1+\mu_{d1}+\alpha_3)(\gamma_2+\mu_{d2}+\alpha_4)-\alpha_3\alpha_4)(\xi_1+\sigma_1)} & \frac{\beta_2\theta_1(\gamma_1+\mu_{d1}+\alpha_3)\sigma_2}{(\theta+\omega_1)((\gamma_1+\mu_{d1}+\alpha_3)(\gamma_2+\mu_{d2}+\alpha_4)-\alpha_3\alpha_4)(\xi_2+\sigma_2)} \end{bmatrix}. \tag{54}$$

The basic reproduction number is found as $R_0 = \max\{R_0^1,\ R_0^2\}$, where $R_0^i\ (i = 1,\ 2)$ denotes the basic reproduction number of each patch. We summarize the result as follows:

Theorem 4. The DFE point of the model (2) is $P^0 = \left(\frac{\theta_1 N_1}{\theta_1+\omega_1},\ \frac{\omega_1 N_1}{\theta_1+\omega_1},\ 0,\ 0,\ \frac{\alpha_1\theta_1 N_1}{\alpha_2(\theta_1+\omega_1)},\ \frac{\alpha_1\omega_1 N_1}{\alpha_2(\theta_1+\omega_1)},\ 0,\ 0\right)$. If $R_0^i < 1,\ i = 1, 2$, then P^0 is locally asymptotic stable. Otherwise, it is unstable.

Proof. We obtain the following system by eliminating V_1 and V_2 in model (2):

$$\begin{aligned}
\frac{dS_1}{dt} &= -\omega_1 S_1 + \theta_1(N_1 - S_1 - E_1 - I_1) + \frac{\beta_1 S_1 I_1}{N_1} - \alpha_1 S_1 + \alpha_2 S_2,\\
\frac{dE_1}{dt} &= \frac{\beta S_1 I_1}{N_1} - \xi_1 E_1 - \sigma_1 E_1,\\
\frac{dI_1}{dt} &= \sigma_1 E_1 - \gamma_1 I_1 - \mu_{d1} I_1 - \alpha_3 I_1 + \alpha_4 I_2,\\
\frac{dS_2}{dt} &= -\omega_2 S_2 + \theta_1(N_2 - S_2 - E_2 - I_2) + \frac{\beta_2 S_2 I_2}{N_2} + \alpha_1 S_1 - \alpha_2 S_2,\\
\frac{dE_2}{dt} &= \frac{\beta S_2 I_2}{N_2} - \xi_2 E_2 - \sigma_2 E_2,\\
\frac{dI_2}{dt} &= \sigma_1 E_2 - \gamma_2 I_2 - \mu_{d2} I_2 + \alpha_3 I_1 - \alpha_4 I_2.
\end{aligned} \tag{55}$$

The Jacobian of Eq.(55) at the point P^0 is obtained as

$$J(P^0) = \begin{bmatrix}
-\omega_1-\theta_1-\alpha_1 & \alpha_2 & -\theta_1 & 0 & -\theta_1-\frac{\beta_1\theta_1}{\theta_1+\omega_1} & 0\\
\alpha_1 & -\omega_2-\theta_2-\alpha_2 & 0 & -\theta_2 & 0 & \frac{-\theta_2-\beta_2\theta_2}{\theta_2+\omega_2}\\
0 & 0 & -\xi_1-\sigma_1 & 0 & \frac{\beta_1\theta_1}{\theta_1+\omega_1} & 0\\
0 & 0 & 0 & -\xi_2-\sigma_2 & 0 & \frac{\beta_2\theta_2}{\theta_2+\omega_2}\\
0 & 0 & \sigma_1 & 0 & -\gamma_1-\mu_{d1}-\alpha_3 & \alpha_4\\
0 & 0 & 0 & \sigma_2 & \alpha_3 & -\gamma_2-\mu_{d2}-\alpha_4
\end{bmatrix}. \tag{56}$$

For P^0 to be stable, it is enough to show that $\det(J(P^0)) > 0$ and $tr(J(P^0)) < 0$. Since all parameters in the model are positive, $tr(J(P^0)) < 0$ from Eq.(56). Now, we apply elementary row operations to obtain the determinant of $J(P^0)$. We observe that

- The first entry on the main diagonal is $(-\omega_1 - \theta_1 - \alpha_1) < 0$.
- The second entry on the main diagonal is $(-\omega_2 - \theta_2 - \alpha_2) + \frac{\alpha_1\alpha_2}{(\omega_1+\theta_1+\alpha_1)} < 0$.
- The third entry on the main diagonal is $-\xi_1 - \sigma_1 < 0$.
- The fourth entry on the main diagonal is $-\xi_2 - \sigma_2 < 0$.
- The fifth entry on the main diagonal is

$$\begin{aligned}
&(-\gamma_1 - \mu_{d1} - \alpha_3) + \frac{\sigma_1\beta_1\theta_1}{(\theta_1+\omega_1)(\xi_1+\sigma_1)}\\
&= \frac{-(\gamma_1+\mu_{d1})(\theta_1+\omega_1)(\xi_1+\sigma_1) + \sigma_1\beta_1\theta_1}{(\theta_1+\omega_1)(\xi_1+\sigma_1)} - \alpha_3\frac{\sigma_1\beta_1\theta_1}{(\theta_1+\omega_1)(\xi_1+\sigma_1)} < 0,
\end{aligned} \tag{57}$$

  where we use the stability condition for the first patch, that is,

$$R_0^1 < 0 \Rightarrow -(\theta_1+\omega_1)(\xi_1+\sigma_1)(\gamma_1+\mu_{d1}) + \beta_1\theta_1\sigma_1 < 0. \tag{58}$$

- The last entry on the main diagonal is rewritten as

$$(-\gamma_2-\mu_{d2}-\alpha_4)+\frac{\sigma_2\beta_2\theta_2}{(\theta_2+\omega_2)(\xi_1+\sigma_2)}-\frac{\alpha_3\alpha_4}{(-\gamma_1-\mu_{d1}-\alpha_3)+\frac{\sigma_1\beta_1\theta_1}{(\theta_1+\omega_1)(\xi_1+\sigma_1)}} \tag{59}$$
$$=(-\gamma_2-\mu_{d2})+\frac{\sigma_2\beta_2\theta_2}{(\theta_2+\omega_2)(\xi_1+\sigma_2)}-\alpha_4\left(1-\frac{\alpha_3}{(\gamma_1+\mu_{d1}+\alpha_3)-\frac{\sigma_1\beta_1\theta_1}{(\theta_1+\omega_1)(\xi_1+\sigma_1)}}\right).$$

Now, we use the stability condition for each patch so that we have

$$R_0^1<1\Rightarrow(\theta_1+\omega_1)(\xi_1+\sigma_1)(\gamma_1+\mu_{d1})-\beta_1\theta_1\sigma_1>0, \tag{60}$$
$$R_0^2<1\Rightarrow(\theta_2+\omega_2)(\xi_2+\sigma_2)(\gamma_2+\mu_{d2})-\beta_2\theta_2\sigma_2>0, \tag{61}$$

with

$$1-\frac{\alpha_3}{(\gamma_1+\mu_{d1}+\alpha_3)-\frac{\sigma_1\beta_1\theta_1}{(\theta_1+\omega_1)(\xi_1+\sigma_1)}}>0. \tag{62}$$

Therefore,

$$(-\gamma_2-\mu_{d2}-\alpha_4)+\frac{\sigma_2\beta_2\theta_2}{(\theta_2+\omega_2)(\xi_1+\sigma_2)}-\frac{\alpha_3\alpha_4}{(-\gamma_1-\mu_{d1}-\alpha_3)+\frac{\sigma_1\beta_1\theta_1}{(\theta_1+\omega_1)(\xi_1+\sigma_1)}}<0. \tag{63}$$

Since all six diagonal entries are negative, their product is positive, which leads to $\det(J(P^0))>0$. If $R_0^i>1$, then the term (59) is positive. Also, the fifth term may change sign on account of the value of α_3. Then, we get an unstable case.

Simulation Results

In this section, we present some simulation results to exemplify the stability theorems, and investigate the effect of the disease transmission rate and migration rate on disease progression. The model equations are solved by the ode23s function of MATLAB [34]. The parameters of the single-patch model are found by data-fitting based on the data of cumulative measles cases in Turkey in 2001 (see Table 1) [27], where we use the function "fminsearchbnd" to estimate the parameters in the optimization step [35]. When we

Table 1. *Distribution of measles cases in Turkey by months in 2001 [27].*

Jan.	Feb.	March	April	May	June	July	Aug.	Sep.	Oct.	Nov.	Dec.
1898	1961	3308	5739	6557	4550	1898	911	679	790	1034	1184

have a look at the number of measles cases and number of deaths in Turkey between 1970 and 2001, it is observed that each outbreak was observed to occur every two years (24 months) to five years (60 months). Therefore, the range in which the mean time to lose immunity is found as $\frac{1}{\theta}\in[\frac{1}{60},\frac{1}{24}]$. Fixing this interval for data-fitting purposes, the mean time to lose immunity is obtained as $\frac{1}{\theta}=0.0351348$ for the available data set. Individuals who become sick can recover between 15 and 30 days, the range of mean duration of infection is obtained as $\frac{1}{\gamma}\in[\frac{30}{30},\frac{30}{15}]=[1,2]$. Then, we estimate $\frac{1}{\gamma}=1.1066$. This result implies that infected individuals will recover approximately in 27 days. The incubation period for measles is about $10-14$ days [36]. Therefore, taking the incubation period of measles in months between 10 and 15 days, the average incubation period lies in the interval $[2,3]$. Similarly, $\frac{1}{\sigma}=2.41388$ is calibrated. This result

indicates that the incubation period of measles is approximately 12 days. We present the values of the parameters in model (1) obtained via data-fitting in Table 2.

Vaccination coverage in 2001 was reported as 84% among children aged 9 months to 5 years [37], where the population of children between 0-14 ages is around 20 million in 2001 [38]. We don't have any information for children between 0-5 ages, so we assume the target group as children between 0-14 ages. As reported in the study [37], vaccination coverage was lower before 2001. Therefore, we assume the initial conditions as $S_0 = 18.000.000$, $V_0 = 2.500.000$, $E_0 = 950$ and $I_0 = 1.898$.

Table 2. *Values of the estimated parameters in Eq.(1).*

Parameter	Description	Value
ω	Rate at which susceptible individuals are vaccinated	0.193956
$\frac{1}{\theta}$	Average time of loosing immunity	0.0351348
β	Transmission coefficient of exposed individuals	2.59105
ξ	Rate of recovery from exposed class due to natural immunity	0.447219
$\frac{1}{\gamma}$	Average length of infection of the infected individuals	1.1066
$\frac{1}{\sigma}$	Average time-span of infected individuals in exposed class	2.41388
$\frac{1}{\mu_d}$	1/ Mortality due to the disease	0.00975329

Simulation Results for the Single-patch Model

By using the parameter values in Table 2, the total number of measles cases obtained from the model (1) and the data given in Table 1 are presented in Figure 3. We observe that our model aligns well with the data meaning that the single-patch model expresses the dynamics well.

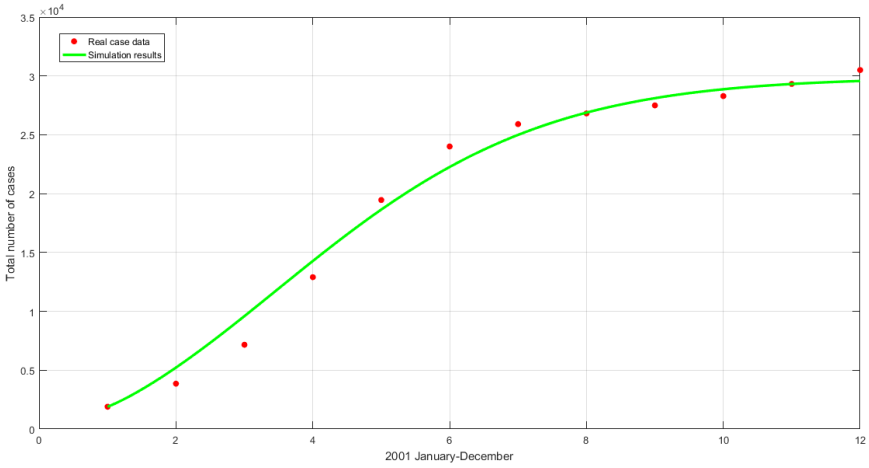

Figure 3. *Simulation results for the number of cumulative measles cases and data points.*

We calculate the DFE point by fixing the size of the population. Then, we will investigate the behaviour of the solution around it. Let us assume that $N = 500$. By using the values in Table 2, we obtain the DFE point $P^0 = (S^0, V^0, 0, 0)$, where $S_0 = \frac{\theta N}{\theta+\omega} \approx 77$ and $V_0 = \frac{\theta N}{\theta+\omega} \approx 423$. Then, the basic reproduction number is calculated as $R_0 \approx 0.3003$. Now, we choose the initial conditions as $S_0 = 79, V_0 = 404, E_0 = 9$ and $I_0 = 8$ for simulation purposes. We observe that S, V, E and I converge to their corresponding values in the DFE P^0 (see Figure 4). The DFE point P^0 is stable since $R_0 < 1$ as we discussed in stability analysis.

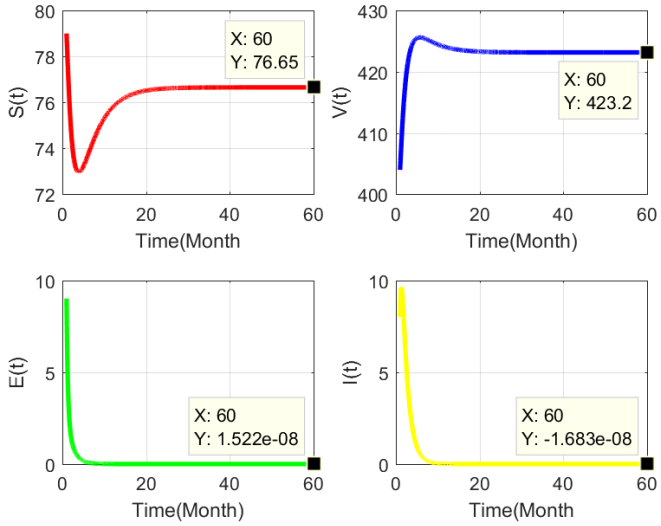

Figure 4. *Simulation results for the single-patch model (1).*

Simulation Results for the Two-patch Model

We fix the values of the additional parameters α_i's and β_i's, since we do not have the data of measles cases for neighboring countries in 2001, whereas we use the values of the other parameters as in Table 1. Simulation results are hypothetical and presented to investigate both the effect of migration or travel rate and transmission coefficient. We fix $\alpha_1 = \alpha_3 = 0.5$, $\alpha_2 = \alpha_4 = 0.4$, $\beta_1 = 2.59105$, $\beta_2 = 2$ and $N_1 = 500$. By using these values, we calculate the DFE point as $P^0 = (S_1^0, V_1^0, 0, 0, S_2^0, V_2^0, 0, 0)$ where $S_1^0 = \frac{\theta_1 N}{\theta_1+\omega_1} \approx 77$, $V_1^0 = \frac{\theta_1 N}{\theta_1+\omega_1} \approx 423$, $S_2^0 = \frac{\alpha_1\theta_1 N}{\alpha_2(\theta_1+\omega_1)} \approx 96$,$V_2^0 = \frac{\alpha_1\theta_1 N}{\alpha_2(\theta_1+\omega_1)} \approx 529$, $N_2 = \frac{\alpha_1 N_1}{\alpha_2} = 625$. Then, the basic reproduction numbers of the patches are $R_0^1 = 0.2677$ and $R_0^2 = 0.1440$ which lead to $R_0 = \max\{R_1, R_2\} = 0.2677$ for the model (2). Choosing the initial conditions as $S_1^0 = 80, V_1^0 = 407, E_1^0 = 7, I_1^0 = 6, S_2^0 = 100, V_2^0 = 508, E_2^0 = 9$ and $I_2^0 = 8$, we simulate the two-patch model for 60 days and present the results in Figure 5. We observe that the variables of two-patch model converge to the DFE point, due to $R_0 < 1$, as expected.
After investigating the consistency of stability analysis with simulation results, we proceed with four different cases listed as:

- **Case 1:** Let $\alpha_1 > \alpha_2 = 0.4, \alpha_3 > \alpha_4 = 0.4, \beta_1 > \beta_2 = 2$.
- **Case 2:** Let $\alpha_1 > \alpha_2 = 0.4, \alpha_3 < \alpha_4 = 0.6, \beta_1 < \beta_2 = 3$.
- **Case 3:** Let $\alpha_1 < \alpha_2 = 0.6, \alpha_3 > \alpha_4 = 0.4, \beta_1 = \beta_2$.
- **Case 4:** Let $\alpha_1 < \alpha_2 = 0.6, \alpha_3 < \alpha_4 = 0.6, \beta_1 = \beta_2$.

The parameters, except those listed above, are fixed as in Table (2). We choose $S_1^0 > S_2^0, V_1^0 > V_2^0, E_1^0 > E_2^0$ and $I_1^0 > I_2^0$. Specifically, we take $S_1^0 = 18.000.000, V_1^0 = 2.500.000, E_1^0 = 950, I_1^0 = 1.898, S_2^0 = 10.000.000, V_2^0 = 1.000.000, E_2^0 = 700$ and $I_2^0 = 1.400$. We present the number of vaccinated individuals in Fig. 6. We observe that both countries reach the same number of vaccinated individuals over time and this behavior is independent of the migration rate between susceptible subgroups (see, Case 1 and Case 2). On the other hand, when the migration of infectious individuals from patch 1 to patch 2 is stronger than the movement in the opposite direction, size of the vaccinated subgroup in

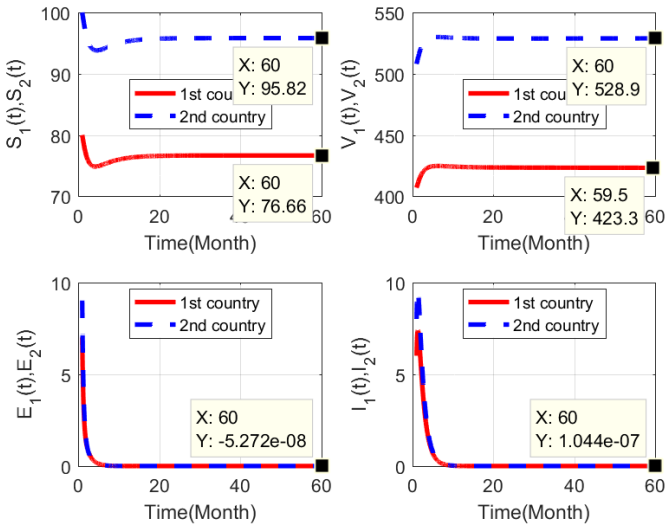

Figure 5. *Simulation results for the two-patch model (2).*

patch 1 increases more than patch 2. Moreover, the number of vaccinated or recovered individuals in both countries are increasing from January to December in all cases as expected due to life-long immunity gained after recovery.

We proceed with the number of infected individuals in Fig. 7. In the beginning of the simulation, the number of infectious individuals is higher in patch 1 than patch 2 in Case 1, but it decreases over time due to life-long immunity and the number of infectious individuals in patch 2 surpasses the same subgroup in patch 1. In Case 2, the migration term of infectious individuals to patch 2 is higher than the one to patch 1 and it leads to a higher peak in patch 2 than patch 1. For Case 3, even though the migration rate of infectious individuals to patch 2 is smaller than the same term to patch 1, the peak of patch 2 is higher than the one for patch 1. It could be due to a higher migration term of the susceptible subgroup to patch 2. Lastly, migration terms in patch 1 are larger than the ones to patch 2, so the peak is higher for patch 2 than patch 1. We see the importance of travel restrictions to control the peak of the spread.

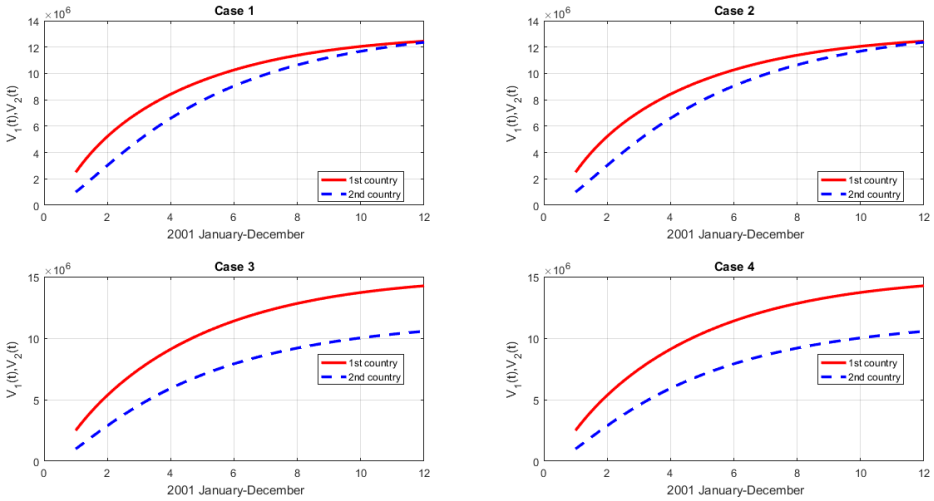

Figure 6. *Comparison of the number of vaccinated/recovered individuals.*

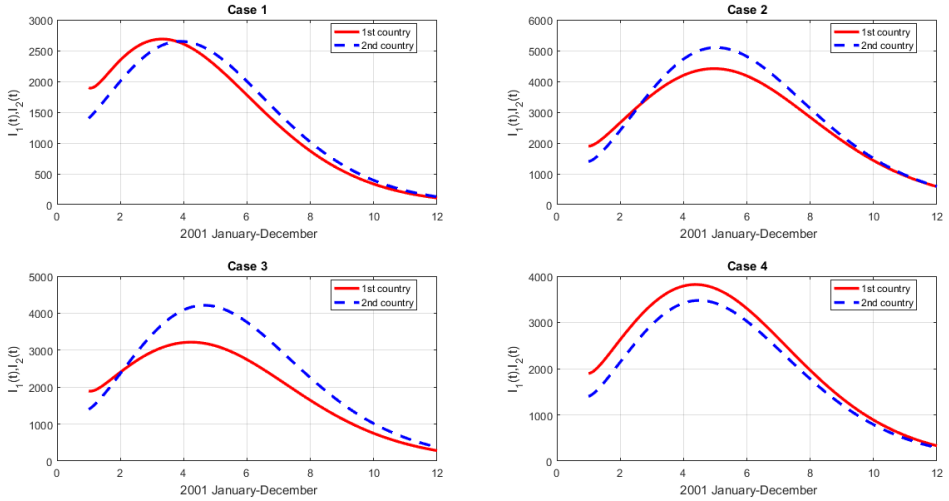

Figure 7. *Comparison of the number of infected individuals.*

Conclusion

In this work, a single-patch mathematical model consisting of susceptible, vaccinated/recovered, latent infected and infected compartments is constructed to investigate progression of measles using the available data of measles cases in Turkey in 2001. The parameters of this model are estimated by data fitting. We observe that simulation results and the data align well. It means that the parameter values found via model calibration are very close to the true values. As the second step, we extend the first model to develop a two-patch mathematical model by including the mutual migration or travel of both susceptible and infectious individuals between two countries. Although this model is based on the data of Turkey, the idea discussed here can be used to model the interaction between any two countries. On the other hand, we find the DFE points and basic reproduction numbers for both models (1)-(2) and we investigate their stability. Finally, we observed that the simulation results are consistent with the theoretical stability analysis. In addition, we investigate the effect of α_i's and β_i's in two-patch model numerically. We observe that both countries reach the same number of vaccinated individuals over time and this behavior is independent of the migration rate between susceptible subgroups. In terms of the number of infectious individuals, numerical results verify the importance of travel restrictions to control the peak of the spread. We acknowledge that our model is simple and incorporates the measles cases recorded only for a year, we believe that the model can be improved for more compartments and larger data sets in the future. In addition, this study can be extended to investigate optimal control strategies.

Declarations

Acknowledgments: This paper is produced from Master Thesis of Turgay Küçük during his studies at Gazi University Thesis number (Council of Higher Education, Thesis Center): 684539
We sincerely thank the anonymous referees for their insightful comments.

Funding/Financial Disclosure: The authors have no received any financial support for the research, authorship, or publication of this study.

Ethics Committee Approval and Permissions: The authors declare that this study did not require approval from an ethics committee or any special permission.

Conflict of Interests: The authors stated that there are no conflict of interest in this article.

Authors Contribution: The authors contributed equally to the study. The authors have read and approved the final version of the article.

Artificial Intelligence (AI): The authors declare that no artificial intelligence (AI) or AI-assisted tools were used in the writing, data analysis, table construction, or figure generation of this article.

References

[1] Akman, T., Köse, E., & Tuncer, N. (2024). Assessment of vaccination and underreporting on COVID-19 infections in Turkey based on effective reproduction number. *International Journal of Biomathematics*, 18(3), 2350102.

[2] Akman Yıldız, T. (2019). A comparison of some control strategies for a non-integer order tuberculosis model. *An International Journal of Optimization and Control: Theories & Applications (IJOCTA)*, *9*(3), 21–30.

[3] Kermack, W. O., & McKendrick, A. G. (1927). A contribution to the mathematical theory of epidemics. *Proceedings of the Royal Society of London Series A, Containing Papers of a Mathematical and Physical Character*, *115*(772), 700–721.

[4] Zhou, X., & Cui, J. (2011). Analysis of stability and bifurcation for an SEIV epidemic model with vaccination and nonlinear incidence rate. *Nonlinear Dynamics*, *63*, 639–653.

[5] Hethcote, H. W. (2000). The mathematics of infectious diseases. *SIAM review*, *42*(4), 599–653.

[6] Li, G.-H., & Zhang, Y.-X. (2017). Dynamic behaviors of a modified SIR model in epidemic diseases using nonlinear incidence and recovery rates. *PLOS ONE*, *12*, 1–28.

[7] Akman Yıldız, T. (2019). Optimal control problem of a non-integer order waterborne pathogen model in case of environmental stressors. *Frontiers in Physics*, *7*, 95.

[8] Akman Yıldız, T., & Karaoğlu, E. (2019). Optimal control strategies for tuberculosis dynamics with exogenous reinfections in case of treatment at home and treatment in hospital. *Nonlinear Dynamics*, *97*, 2643–2659.

[9] Akbari, R. (2023). An investigation into the optimal control of the horizontal and vertical incidence of communicable infectious diseases in society. *Journal of Mathematical Modeling*, *11*(4), 605–616.

[10] Babayar-Razlighi, B. (2023). Numerical solution of an influenza model with vaccination and antiviral treatment by the Newton-Chebyshev polynomial method. *Journal of Mathematical Modeling*, *11*(1), 103–116.

[11] Yang, W. (2021). Dynamical behaviors and optimal control problem of an SEIRS epidemic model with interventions. *Bulletin of the Malaysian Mathematical Sciences Society*, *44*(5), 2737–2752.

[12] Gürbüz, B., & Gökçe, A. (2022). An algorithm and stability approach for the acute inflammatory response dynamic model. In Operations Research, CRC Press, 192–217.

[13] Griffin, D. (1995). Immune responses during measles virus infection. *Measles virus*, 117–134.

[14] Krugman, S., Giles, J. P., Friedman, H., & Stone, S. (1965). Studies on immunity to measles. *The Journal of pediatrics*, *66*(3), 471–488.

[15] Bester, J. C. (2016). Measles and measles vaccination: a review. *JAMA pediatrics*, *170*(12), 1209–1215.

[16] Edward, S., Raymond, K., Gabriel, K., Nestory, F., Godfrey, M., & Arbogast, M. (2015). A mathematical model for control and elimination of the transmission dynamics of measles. *Applied and Computational Mathematics*, *4*(6), 396–408.

[17] Gürbüz, B., Hatipoğlu, V. F., & Gökçe, A. (2024). A numerical approach for a dynamical system of fractional infectious disease problem. *Hacettepe Journal of Mathematics and Statistics*, *53*(6), 1542-1559.

[18] Isik, O. R., Tuncer, N., & Martcheva, M. (2024). Mathematical model of measles in Turkey. *Journal of Biological Systems*, *32*(3), 941-970.

[19] Akman, T. (2025). Identifiability Analysis of a Mathematical Model for the First Wave of COVID-19 in Türkiye. *Bitlis Eren Üniversitesi Fen Bilimleri Dergisi*, *14*(1), 494-512.

[20] Roberts, M., & Tobias, M. (2000). Predicting and preventing measles epidemics in New Zealand: application of a mathematical model. *Epidemiology & Infection*, *124*(2), 279–287.

[21] Garba, S., Safi, M., & Usaini, S. (2017). Mathematical model for assessing the impact of vaccination and treatment on measles transmission dynamics. *Mathematical Methods in the Applied Sciences*, *40*(18), 6371–6388.

[22] Ibrahim, M. A., & Dénes, A. (2023). Stability and threshold dynamics in a seasonal mathematical model for measles outbreaks with double-dose vaccination. *Mathematics*, *11*(8), 1791.

[23] Duncan, S., Scott, S., & Duncan, C. (1999). A demographic model of measles epidemics. *European Journal of Population/Revue européenne de Démographie*, *15*, 185–198.

[24] Kuddus, M. A., Mohiuddin, M., & Rahman, A. (2021). Mathematical analysis of a measles transmission dynamics model in Bangladesh with double dose vaccination. *Scientific reports*, *11*(1), 16571.

[25] Nie, J., Chen, Q., Teng, Z., Zhang, Y., & Rifhat, R. (2024). Dynamics of a stochastic measles model with general incidence rate and Black–Karasinski process. *Bulletin of the Malaysian Mathematical Sciences Society*, *47*(6), 175.

[26] Sahu, G. P., & Dhar, J. (2012). Analysis of an SVEIS epidemic model with partial temporary immunity and saturation incidence rate. *Applied Mathematical Modelling*, *36*(3), 908–923.

[27] Kara, I., Ceylan, A., & Acemoglu, H. (2004). Measles epidemics in Turkey and developing countries: Review of the literature. *Middle East Journal of Family Medicine*, *5*, 1–11.

[28] Tewa, J. J., Bowong, S., & Mewoli, B. (2012). Mathematical analysis of two-patch model for the dynamical transmission of tuberculosis. *Applied Mathematical Modelling*, *36*(6), 2466–2485.

[29] Bianchi, F. P., Mascipinto, S., Stefanizzi, P., De Nitto, S., Germinario, C., & Tafuri, S. (2021). Long-term immunogenicity after measles vaccine vs. wild infection: An Italian retrospective cohort study. *Human Vaccines & Immunotherapeutics*, *17*(7), 2078–2084.

[30] Griffin, D. E. (2016). The immune response in measles: virus control, clearance and protective immunity. *Viruses*, *8*(10), 282.

[31] Wessel, L. (2016). Impact of vaccination and mobility on disease dynamics: a two patch model for measles. Master's thesis, Department of Mathematics, University of Manitoba, Winnipeg.

[32] Dreessche, P., & Watmough, J. (2002). Reproduction numbers and sub-threshold endemic equilibria for compartmental models of disease transmission. *Mathematical Biosciences*, *180*, 29–48.

[33] Salmani, M., & van den Driessche, P. (2006). A model for disease transmission in a patchy environment. *Discrete and Continuous Dynamical Systems - B*, *6*(1), 185–202.

[34] The MathWorks, Inc., *MATLAB version: 9.8 (R2020a)*, Natick, Massachusetts: The MathWorks, Inc., 2020. [Online]. Available: `https://www.mathworks.com`.

[35] J. D'Errico, *fminsearchbnd, fminsearchcon*, MATLAB Central File Exchange, 2025. [Online]. Available: `https://www.mathworks.com/matlabcentral/fileexchange/8277-fminsearchbnd-fminsearchcon`. [Accessed: 1-Jan-2021].

[36] Memon, Z., Qureshi, S., & Memon, B. R. (2020). Mathematical analysis for a new nonlinear measles epidemiological system using real incidence data from pakistan. *The European Physical Journal Plus*, *135*(4), 378.

[37] Güriş, D., Bayazıt, Y., Özdemirer, Ü., Buyurgan, V., Yalnız, C., Toprak, İ., & Aycan, S. (2003). Measles epidemiology and elimination strategies in Turkey. *Journal of Infectious Diseases*, *187*(Supplement_1), S230–S234.

[38] World Bank, *Population ages 0-14 (% of total population) - Turkiye*, World Development Indicators, 2024. [Online]. Available: `https://data.worldbank.org/indicator/SP.POP.0014.TO.ZS?locations=TR`. [Accessed: 15-May-2023].